

# SOVIET PHYSICS

## JETP

*A translation of the Journal of Experimental and Theoretical Physics of the USSR.*

SOVIET PHYSICS JETP

VOL. 35 (8), NO. 1, pp 1-216

JANUARY, 1959

### INTERACTION OF COSMIC RAY PARTICLES WITH VARIOUS NUCLEI

N. L. GRIGOROV, A. V. PODGURSKAIA, A. I. SAVEL' EVA, and L. M. POPEREKOVA

Submitted to JETP editor September 27, 1956; resubmitted March 25, 1958

J. Exptl. Theoret. Phys. (U.S.S.R.) 35, 3-15 (July, 1958)

The transition effect of stars and single heavily ionizing particles was studied by means of nuclear emulsions exposed at the altitudes of 20 and 9 km under various absorbers. The results indicate that the multiplicity and mean disintegration energy of the stars are proportional to  $A^{1/3}$ . Data on the flux and spectrum of heavily ionizing particles in air and under lead absorbers make it possible to analyze earlier results<sup>1</sup> on the production of  $\pi^0$  mesons in lead and air. It is shown that the mean energy carried away by  $\pi^0$  mesons produced in interactions of  $\sim 10^{10}$  ev cosmic ray primaries with nuclei is proportional to the radius of the target nucleus.

#### INTRODUCTION

WE have determined the average characteristics of the interaction between primary cosmic ray particles of  $\sim 10^{10}$  ev energy and light nuclei through the study of the various secondary components of cosmic radiation observed in the atmosphere.<sup>2</sup>

We have studied the dependence of star energy and multiplicity on the atomic number of the disintegrating nucleus, in order to find out to which extent these characteristics depend on the size of the target nucleus. Moreover, having investigated the variation of the flux of heavily-ionizing particles and the ionization due to these in air and under lead absorbers of various thickness, we found it possible to determine the energy carried away by  $\pi^0$  mesons produced in lead, and, comparing its value with the energy of  $\pi^0$  mesons produced in air, to draw conclusions regarding meson production in light and heavy nuclei; this could be done by a more correct method than that used earlier.<sup>1</sup>

Our method of determining the energy of a nuclear disintegration is based on the following considerations: As the result of disintegration, the nucleus emits heavy charged particles that carry away an average energy  $E_C$ . The major portion

of these particles have a range considerably smaller than the absorption mean free path of the star-producing component. Under a sufficiently thick layer  $x$  of matter ( $x < R$ , where  $R$  is the range of secondary particles produced in nuclear disintegrations), an equilibrium is reached between the secondary and primary particles. Then the charged products of nuclear disintegrations lose in one gram of matter, an amount of energy equal to that gained, in one gram, from all nuclear disintegrations. To determine  $E_C$ , it is therefore necessary to measure the total ionization produced per unit volume by all heavily-ionizing particles. Let  $N(I, \theta) dI d\Omega$  represent the number of particles with specific ionization  $I$  to  $I + dI$ , traveling at zenith angle  $\theta$  in a solid angle  $d\Omega$ . The ionization energy loss in one gram of matter, suffered by all particles, is then

$$\frac{\Delta E}{\Delta x} = \beta_{\text{rel}} \int_{\Omega} d\Omega \int_{I_{\text{min}}}^{\infty} \frac{I}{I_{\text{rel}}} N(I, \theta) dI, \quad (1)$$

where  $\beta_{\text{rel}}$  is the relativistic ionization loss per gram of the given substance for relativistic particles with ionization  $I_{\text{rel}}$ . For the equilibrium conditions

$$E_c = (\Delta E / \Delta x) L_i / S,$$

where  $S$  is the flux of the star-producing component and  $L_i$  is the interaction mean free path for the given substance.

If the energy  $E_c$  transferred to charged products of nuclear disintegration is known, the total energy of disintegration  $E_t$  can be found under the assumption that the neutrons carry away an amount of energy  $(A - Z)/Z$  times larger than that carried away by the protons. Since, according to reference 3, the main fraction of energy is carried away by protons, we have

$$E_t = AE_c / Z. \quad (2)$$

## 1. EXPERIMENTAL RESULTS

Emulsions were chosen for the measurement of the ionization due to heavily-ionizing particles, in view of good identification of particles through their specific ionization.

As stated in the Introduction, to determine  $E_t$  we had to measure the particle spectrum  $N(I, \theta) dI d\Omega$  under absorbers of sufficient thickness, made of materials with different atomic number. The experiments were carried out at the geomagnetic latitude  $51^\circ$ , using graphite and lead absorbers of various thickness at an altitude of 20 km, and using lead and paraffin absorbers at 9 km altitude.

Electron-sensitive emulsions  $400 \mu$  thick were used in the stratospheric experiments. One part of the plates,  $4 \times 4$  cm, was placed under flat lead absorbers I, II and III (cf. Fig. 1a), 5, 15, and 33 mm in thickness respectively. Another part of the plates, also  $4 \times 4$  cm in size, was placed between flat graphite absorbers IV, V, and XI, 13, 39, and 86 mm in thickness. Lead and graphite absorbers were placed together with the plates in hermetic copper cassettes with walls 0.5 mm thick (cf. Fig. 1a). A pair of plates wrapped in a single layer of paper was placed back to back under each filter. The plates were placed in a vertical plane. Two hermetic brass cassettes VII and VIII, with walls 0.3 mm thick and containing a pair of  $6 \times 9$  cm plates without absorbers, were used in addition. One of these cassettes was placed in the array, at a distance of  $\sim 40$  cm from the cassettes containing the lead and graphite absorbers. The other was hung 4 m above the array. All cassettes were filled with pure argon at atmospheric pressure.

A diagram of the flight and position of the cassettes in the array are shown in Fig. 1, b and c.

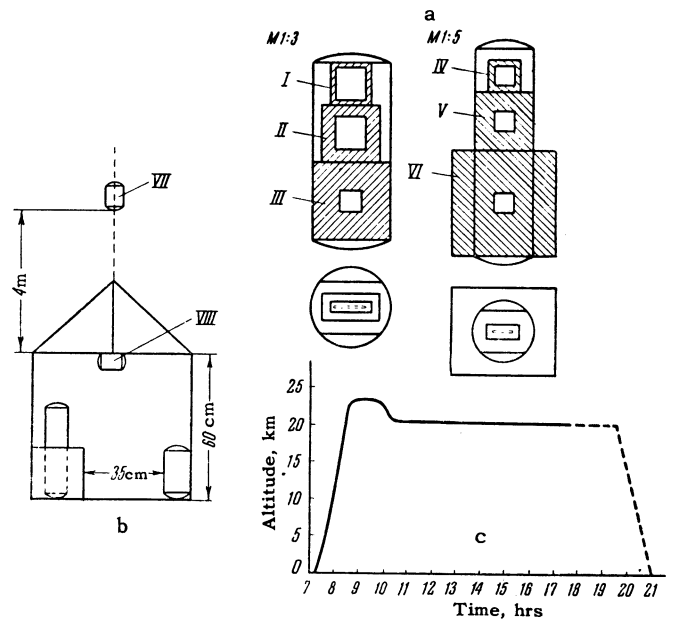


FIG. 1. a - position of nuclear emulsion plates in the cassettes under graphite and lead absorbers in the stratospheric experiment, b - position of the cassettes in the array, c - flight diagram.

The altitude was monitored by radio during the flight. The radio communication stopped 11 hrs after the start. This happened at the altitude of 20 km. The apparatus landed after 21 hours. Assuming that the apparatus descended with the same velocity as it ascended (which is true in most cases), then the array spent about 11 hours at altitude  $\geq 20$  km (cf. flight diagram, Fig. 1c; the inferred part of the flight is indicated by the dotted line). In the following, the time of flight at 20 km is taken as  $\sim 11$  hours.

Electron-sensitive emulsions  $600 \mu$  in thickness were used in the experiments at 9 km altitude. Eight  $5 \times 10$  cm plates (4 in each cassette) were placed in two hermetic brass cassettes with walls 0.3 mm thick, filled with argon at atmospheric pressure. One cassette was placed in a lead cylinder, with side walls 3.5 cm thick. The other cassette was placed in a paraffin vessel of the same form with walls 17 cm thick. The plates in both cassettes were exposed in a vertical position.

The emulsions were exposed in an airplane during a month. The total time spent at 9 km altitude amounted to 25 hours.

In scanning, we measured (a) the total number of stars with  $N_h \geq 3$  under various absorbers, (b) the number of single heavily-ionizing particles stopping in the emulsion, and (c) the number of single heavily-ionizing particles traversing the emulsion, and their angular as well as specific ionization distribution.

## 2. STARS UNDER VARIOUS ABSORBERS

The data on the number of stars under various absorbers, given in Table I, represent the mean of two scanings of each plate by several observers. The standard deviation of the measurements of the number of stars by different observers was found to be 5 to 6% (two times larger than the statistical error).

TABLE I

Altitude, km	Material and thickness of the absorber, mm	Number of stars $\text{cm}^{-3} \text{ day}^{-1}$
20	Air	2350
	Graphite 13	1910
	" 39	2520
	" 86	2190
	Lead 5	2130
	" 15	2360
9	" 33	2430
	Paraffin 170	402
	Lead 35	417

It can be seen from Table I that, within the limits of experimental errors, amounting to 6%, the number of stars found in the plates exposed at 9 and 20 km altitude is independent of the material of the absorber surrounding the emulsion.

## 3. HEAVILY IONIZING PARTICLES UNDER VARIOUS ABSORBERS

The plates were scanned for stopping heavily ionizing particles at  $450\times$  magnification. Each field of view was scanned in the whole depth of the emulsion. We measured the angle  $\theta$  between the projection of the track on the plane of the plate and the vertical, the dip of the track, and its length (from the point of entrance into the emulsion to the point where the particle stopped).

The plates were scanned for particles traversing the emulsion at  $2020\times$  magnification. The scanning was carried out along the surface (at the depth of a few microns). All tracks with grain density  $g \gtrsim 2g_{\text{min}}$  and a length of projection on the emulsion plane  $l \geq 800\mu$  were noted in the scanning. For tracks traversing the emulsion and satisfying these above conditions, we measured the length  $l$  of projection on the emulsion-plane, the grain density  $g$ , and the angle  $\theta$  between the projection and the vertical.

It was not possible to determine the direction of motion of the particle along the track when the particle did not stop in the emulsion. The angular distribution of these particles about the vertical

was therefore measured in the range from 0 to  $90^\circ$ . The number of inspected fields of view and the number of particles found in them were noted in the scanning for stopping and traversing particles.

The angular distribution of the traversing particles at 20 and 9 km altitude is shown in Fig. 2.

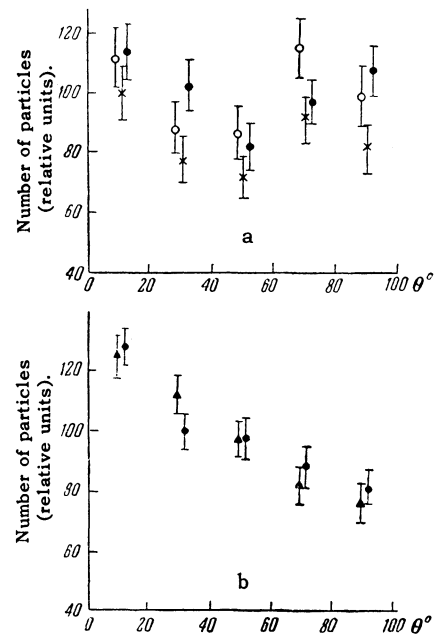


FIG. 2. Angular distribution of heavily ionizing particles, non-stopping in the emulsion, under various absorbers: a – at 20 km altitude, b – at 9 km altitude. The x axis represents the angle between the projection of the track on the plane of emulsion and the vertical, and the y axis the number of particles between 0 and  $20^\circ$ . Absorbers: x – graphite, o – air, ● – lead, ▲ – paraffin.

The angular distribution of particles, recorded in emulsions exposed at 20 km altitude in air, has been plotted from 549 tracks, that under 86 mm of graphite from 549 tracks, and that under 33 mm of lead from 670 tracks. These distributions are normalized in Fig. 2 to the same number of detected particles. The angular distribution of traversing particles in plates exposed at 9 km altitude under 170 mm of paraffin has been plotted from 1240 tracks, and that under 35 mm of lead from 1212 tracks.

It can be seen from Fig. 2 that the angular distributions of traversing particles are practically identical under absorbers of small or large atomic number (air, graphite, and lead at 20 km altitude, paraffin and lead at 9 km). At 20 km, the angular distribution of tracks traversing the emulsion is practically isotropic. At 9 km, the angular distribution of the particles is slightly anisotropic, evidently owing to the greater anisotropy of the star-producing component.

TABLE II

Altitude, km	Absorber	Range of angles								
		0-20°	20-40°	40-60°	60-80°	80-100°	100-120°	120-140°	140-160°	160-180°
20	Air	79±5	59±4	63±5	61±5	64±5	53±4	45±4	48±4	44±4
20	Graphite	76±5	69±6	69±6	63±6	69±6	51±5	36±4	30±4	37±4
20	Lead	65±6	57±5	57±5	61±6	61±6	52±5	46±5	45±5	50±5
9	Paraffin	78±11	70±11	70±11	70±11	47±8	50±9	44±8	45±9	27±6
9	Lead	103±9	74±8	66±7	66±7	47±6	41±6	44±6	35±5	33±5

TABLE III

Altitude		20 km (400 μ emulsion)			9 km (600 μ emulsion)	
Absorber		Air	Graphite, 86 mm	Lead, 33 mm	Paraffin, 170 mm	Lead, 35 mm
Number of stars, cm <sup>-3</sup> day <sup>-1</sup>		2350±120*	2190±120*	2430±120*	402±8	417±12
Stopping particles	Number of particles stopping in 1 cm <sup>2</sup> per minute	0.110±0.005	0.141±0.007	0.162±0.009	0.075±0.004	0.0.5±0.004
	Flux of particles 6 Mev ≤ E ≤ 20 Mev, cm <sup>-2</sup> sterad <sup>-1</sup>	0.069±0.006	0.058±0.005	0.085±0.006	0.023±0.0015	0.024±0.0015
Flux of traversing particles 20 Mev ≤ E ≤ 180 Mev, cm <sup>-2</sup> min <sup>-1</sup> sterad <sup>-1</sup>		2.5±0.1	2.5±0.1	2.8±0.3	0.34±0.01	0.38±0.01

\*The error represents the standard deviation, amounting to 6% of the measured value.

Results of the measurements of the angular distribution of stopping particles are given in Table II. The distribution is normalized to the same total number of particles detected under various absorbers.

In certain cases, the mass of heavily ionizing particles traversing the emulsion was determined by multiple scattering and grain-density measurements. These non-systematic measurements have shown that, both in the atmosphere and under lead, the majority of traversing particles are protons. It was possible, therefore, to obtain the energy distribution of these particles from the measured grain density, assuming they were all protons.

It is evident that the energy spectrum of the detected particles traversing the emulsion will differ from the true spectrum since, for particles with different grain density  $g$ , the solid angle within which they are classified as having trav-

ersed the emulsion will be different.

In addition, the true value of grain density is different from that observed in its dependence on the angle of dip of the track with respect to the plane of emulsion. Corresponding corrections were applied to the energy spectrum of traversing particles. The spectra represented by the histograms in Fig. 3 (for 20 km altitude) and Fig. 4 (for 9 km) were obtained as the result. Experimental points are shown in the figures.

It can be seen from Fig. 3 and 4 that the energy spectrum of traversing particles is practically independent of the atomic number of the absorber, at both altitudes, 20 km and 9 km. The values of the flux of traversing particles, accounting for the corrections, are given in Table III (4th column).

The energy spectrum of stopping particles was determined from the measured range spectrum,

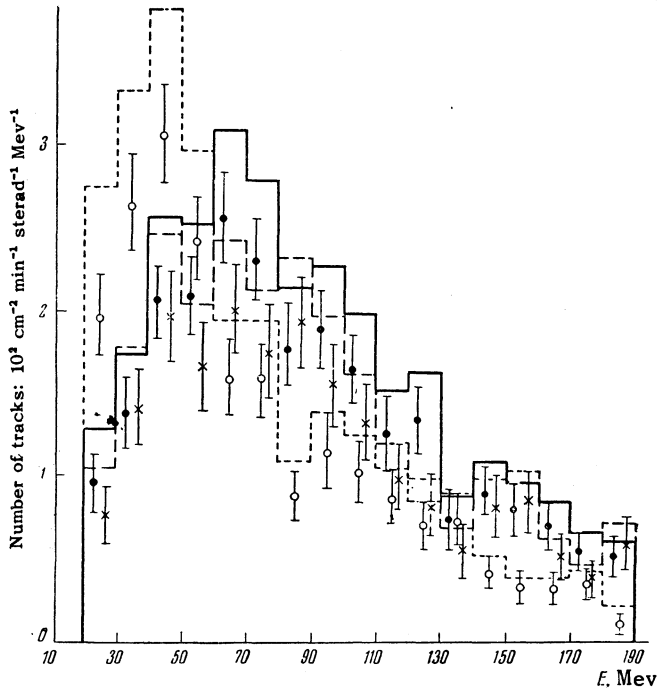


FIG. 3. Energy spectrum of heavily-ionizing particles traversing the emulsion (all particles are assumed to be protons) at 20 km altitude. The x axis represents the particle energy, and the y axis the flux of particles with a given energy under various absorbers:  $\times$  - graphite,  $\circ$  - air,  $\bullet$  - lead.

under the assumption that all particles were protons. In constructing the spectrum, we took it into account that the finite thickness of the emulsion distorts considerably the true range distribution. After introducing a corresponding correction, the energy spectrum of stopping particles was found to be identical under all absorbers, within the limits of statistical errors of the measurements. In the energy range  $6 \text{ Mev} \leq E \leq 20 \text{ Mev}$ , the spectrum is

$$N(E)dE = \text{const } dE.$$

The absolute intensity of the flux of stopping particles is given in Table III (3rd column). It can be seen that when the plates were surrounded by a layer of lead 3.3 to 3.5 cm thick (effective thickness 5 to 6 cm), the number of stars and of single particles remained practically constant at both elevations.

#### 4. PRODUCTION OF $\pi^0$ MESONS IN SUBSTANCES WITH DIFFERENT ATOMIC NUMBER

Information can be gained on the production of  $\pi^0$  mesons by cosmic ray particles in light (air) and heavy (lead) substances, comparing the energy  $\epsilon_{\pi^0}$  carried away by  $\pi^0$  mesons per second in one gram of air and lead at the same observa-

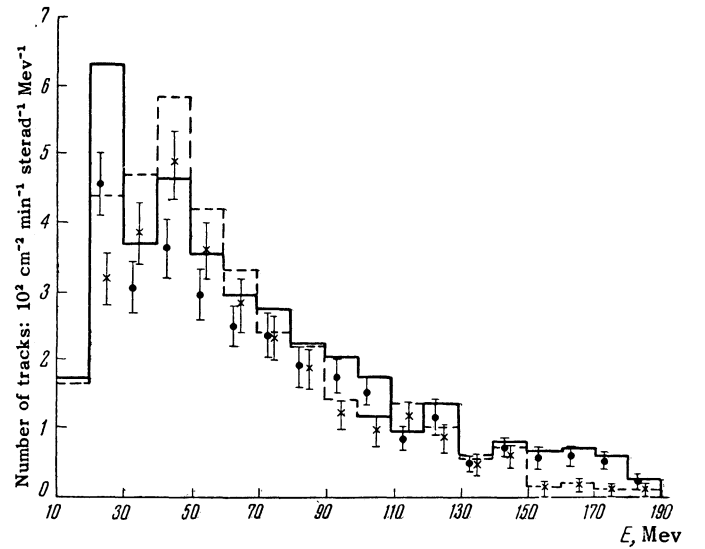


FIG. 4. Energy spectrum of heavily ionizing particles traversing the emulsion, at 9 km altitude, under various absorbers:  $\times$  - paraffin,  $\bullet$  - lead.

tion level, for equal intensity and properties of the producing component. If we denote the mean value of energy carried away by  $\pi^0$  mesons in one interaction of the generating particle with air and lead nuclei by  $E_{\pi^0}^{\text{Air}}$  and  $E_{\pi^0}^{\text{Pb}}$  respectively, then we have the following relation between  $\epsilon$  and  $E$ :

$$\epsilon_{\pi^0}^{\text{Air}} = E_{\pi^0}^{\text{Air}} P / L_{\text{Air}}, \quad \epsilon_{\pi^0}^{\text{Pb}} = E_{\pi^0}^{\text{Pb}} P / L_{\text{Pb}},$$

where  $L_{\text{Air}}$  and  $L_{\text{Pb}}$  are the interactions mean free paths of the generating particles in air and lead, respectively, and  $P$  is the total flux of these particles. Eliminating  $P$ , we obtain

$$E_{\pi^0}^{\text{Pb}} / E_{\pi^0}^{\text{Air}} = \epsilon_{\pi^0}^{\text{Pb}} L_{\text{Pb}} / \epsilon_{\pi^0}^{\text{Air}} L_{\text{Air}}. \quad (3)$$

The value of  $\epsilon_{\pi^0}^{\text{Air}}$  can be determined in the following way: The energy  $\epsilon_{\text{SC}}(x)$  transferred to the soft component per second and per gram at atmospheric depth  $x \text{ g/cm}^2$ , is related to the energy flux  $S^{\text{H}}(x)$  carried by the soft component through  $1 \text{ cm}^2$  of horizontal surface and to the total flux of soft component  $N_{\text{SC}}(x)$  by the expression<sup>1</sup>

$$\frac{dS^{\text{H}}(x)}{dx} + \beta N_{\text{SC}}(x) = \epsilon_{\text{SC}}(x). \quad (4)$$

where  $\beta = C - dE(dx)_{\text{ion}}$  is the ionization loss for relativistic electrons.

We determined  $\epsilon_{\text{SC}}(x)$  using data of references 1, 2, and 4. The dependence of  $\epsilon_{\text{SC}}(x)$  on the atmospheric depth  $x$  is shown in Fig. 5. Curve 1 refers to measurements at  $31^\circ$  geomagnetic latitude, where the energy of primary cosmic ray particles is  $E_0 \geq 7 \text{ Bev}$ . Curve 2 represents the difference of measurements at  $51^\circ$  and  $31^\circ$  geomagnetic latitude ( $1.5 \text{ Bev} \leq E_0 < 7 \text{ Bev}$ ).

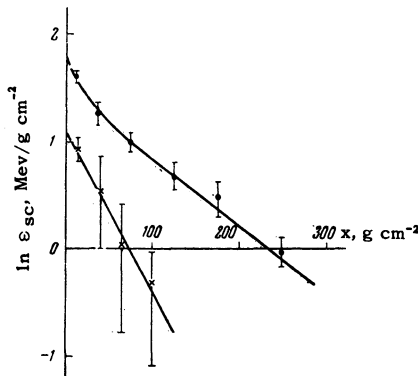


FIG. 5. Dependence of the energy transferred into the soft component in 1g of air,  $\epsilon_{sc}$  on the atmospheric depth  $x$ : ● - for primaries with  $E_0 \leq 7$  Bev, × - for primaries with  $1.5 \leq E_0 \leq 7$  Bev.

Correcting  $\epsilon_{sc}(x)$  for the contribution of electrons originating in the  $\mu$ -meson decay, we obtain the energy carried away by  $\pi^0$  mesons in one gram of atmosphere, i.e.,  $\epsilon_{\pi^0}^{Air}$ . Corresponding values of  $\epsilon_{\pi^0}^{Air}$  are given in the fifth column of Tables IV and V.

The energy  $\epsilon_{\pi^0}^{Pb}$  carried away by  $\pi^0$  mesons in one gram of lead per second can be determined from the following considerations. If  $n(t)$  represents the number of electrons under a thickness of lead  $t$ , originating in the decay of  $\pi^0$  mesons produced in it, then the energy transferred to  $\pi^0$  mesons in one gram of lead can be found from the equation

$$n(t) = \epsilon_{\pi^0}^{Pb} \exp\{-t/L_{Pb}\} \gamma(t)/\beta_{Pb}, \quad (5)$$

where  $L_{Pb} = 160 \text{ g/cm}^2$  is the interaction mean free path of nuclear active particles in lead,  $\beta_{Pb} = 1.2 \text{ Mev-g}^{-1} \text{ cm}^2$  is the ionization loss suffered by relativistic electrons in lead, and

$$\gamma(t) = \int_0^t N(\xi) \exp\{\xi/L_{Pb}\} d\xi / \int_0^\infty N(\xi) d\xi,$$

where  $N(\xi)$  is the mean number of particles at the depth  $\xi$  in showers produced by  $\pi^0$ -decay photons.

From Eq. (5) we have

$$\epsilon_{\pi^0}^{Pb} = n(t) \beta_{Pb} / \gamma(t) \exp\{-t/L_{Pb}\}. \quad (6)$$

It can be seen from Eq. (6) that in order to find  $\epsilon_{\pi^0}^{Pb}$ , it is necessary to measure the total flux of particles  $n(t)$  of the soft component under the lead absorber in which it is produced. The particles measured should not include any particles due to the electron-photon component incident upon the lead absorber.

The number of particles under a lead absorber 8 cm thick (effective thickness  $\sim 9$  cm) was meas-

ured in a series of experiments at  $51^\circ$  N geomagnetic latitude.<sup>2</sup> It is evident that in that experiment the soft component incident from the atmosphere was practically all absorbed. Consequently, the difference between  $N_8$ , the measured number of particles under 8 cm of lead, and  $N_{hc}$ , the total flux of the hard component, gives the flux of secondary particles produced in the lead by the nuclear-active component. This relation can be approximated by  $N_8 - N_{hc} = Ae^{-x/\lambda}$ , where  $\lambda = 80 \pm 17 \text{ g/cm}^2$ .

The number of particles and the ionization in air under lead absorbers 1, 2, and 4 cm thick were measured in another series of experiments carried out at  $31^\circ$  and  $51^\circ$  N geomagnetic latitude.<sup>2</sup> The results show that, at any altitude, the maximum of the air-lead transition curve lies between 1 and 2 cm of lead. The value of the transition-curve maximum (related to one particle of the soft component incident upon the lead absorber) varies by merely 20% only as  $x$  changes from 310 to 40  $\text{g/cm}^2$ . It follows that the mean energy of the particles of the soft component in the atmosphere is practically independent of the depth of observation, and that the transition curves should be similar at all altitudes.

The value of the mean energy is such that the air-lead transition curve for 4 cm of lead ( $\sim 4.7$  cm effective thickness), has an ordinate equal to the flux of charged particles of the soft component (cf. the transition curve for  $x = 310 \text{ g/cm}^2$  in Fig. 6 of reference 2). At high altitudes, however, the air-lead transition curve becomes distorted: particles not present under the absorber at low altitudes begin to appear (cf. Fig. 6 of reference 2). These particles are due to the production of  $\pi^0$  mesons in the absorber. The flux of the "additional" particles, equal to  $N_4 - N_0$  (where  $N_4$  is the flux of particles under an absorber in the atmosphere) determines the required value  $n(t)$ . Certain corrections, which will be discussed below, have to be applied to the calculation.

The  $y$  axis in Fig. 6 represents the difference  $N_4 - N_0$  measured at various depths  $x$  in the atmosphere at two geomagnetic latitudes. It can be seen from Fig. 6 that the number of the "additional" particles under 4 cm of lead is, at all altitudes, the same as under 8 cm of lead ( $N_8 - N_{hc}$ ). (The calculation shows that, in cascades initiated by  $3 \times 10^8$  to  $10^9$  ev photons originating in the decay of  $\pi^0$  mesons produced in lead, the number of particles under 8 cm Pb is only 20% higher than that under 4 cm Pb.) At high altitudes, the flux of the "additional" particles under 4 cm Pb equals  $\sim 1.5 \text{ cm}^{-2} \text{ sec}^{-1}$ . If we assume that the interac-

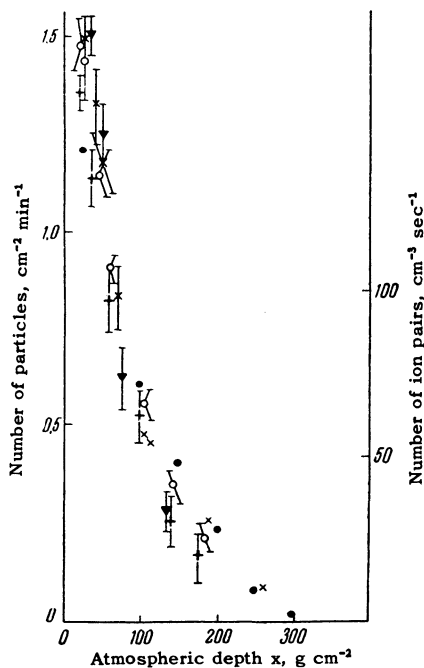


FIG. 6. Dependence of the number of electrons (left-hand scale) originating in the  $\pi^0$  mesons produced, and the ionization due to them (right-hand scale), on the atmospheric depth  $x$ . Results of measurements at  $51^\circ\text{N}$  geomagnetic latitude:  $\blacktriangledown$ :  $N_8 - N_{\text{HC}}$ ,  $\circ$ :  $N_4 - N_0$ ,  $\bullet$ :  $I_4 - I_0$ ; results of measurements at  $31^\circ\text{N}$  latitude:  $+$ :  $N_4 - N_0$ ,  $\times$ :  $I_4 - I_0$ .

tion mean free path of the generating particles in lead equals  $160 \text{ g/cm}^2$  and that the total flux of these particles decreases with the atmospheric depth as the mean free path  $\lambda = 80 + 17 \text{ g/cm}^2$ , we find that, in the mean, 60 secondary particles are emitted from the 4 cm layer of lead in each interaction between a primary with energy  $\geq 7 \text{ Bev}$  ( $\bar{E}_0 \approx 20 \text{ Bev}$ ) and a lead nucleus. It is clear that the majority of these particles are electrons, produced in lead as the result of cascade multiplication.

If the air-lead transition effect is measured by means of an ionization chamber, then the difference between ionization  $I_4$  measured under a lead absorber 4 cm thick, and that measured in the atmosphere,  $I_0$ , represents the ionization due to photons from the decay of  $\pi^0$  mesons produced in the absorber. The dependence of  $I_4 - I_0$  on  $x$  is shown in Fig. 6 (the scale for  $I_4 - I_0$  is given on the right-hand-side).

The ratio  $(I_4 - I_0)/(N_4 - N_0) = \bar{K}$  represents the mean specific ionization of the "additional" particles. It follows from Fig. 6, that, at all altitudes,  $\bar{K} = 120 \text{ ion pairs/cm}$ , which is 1.7 times the specific ionization of fast electrons ( $70 \text{ ion pairs/cm}$ ).<sup>5</sup> This increase of the specific ionization is due to two causes: (a) errors in the number of particles measured under the lead absorber

(owing to finite dimensions of the counter), and (b) the presence there of slow electrons, which undergo large scattering within the volume of the chamber and which suffer, therefore, a larger energy loss  $(dE/dx)_{\text{ion}}$ .

Our measurements of the transition effect of heavily-ionizing particles indicate that the flux and spectrum of these particles are identical in air and under 4 cm of lead. The total ionization due to heavily-ionizing particles is, therefore, also identical for both conditions. In consequence, the increase in the specific ionization under 4 cm Pb cannot be ascribed to the heavily-ionizing particles.

In Eq. (6),  $n(t)$  is the true number of electrons under a lead absorber of thickness  $t$ , and  $\beta$  is the average ionization loss in lead. If we determine  $\epsilon_{\pi^0}^{\text{Pb}}$  by using the number of particles observed and putting  $\beta_{\text{Pb}} = 1.2 \text{ Mev/g-cm}^{-2}$  for relativistic particles, then, in order to obtain the correct value of  $n(t)_{\text{obs}} \beta_{\text{Pb}}$ , it is necessary to multiply it by the factor 1.7, which accounts automatically both for the error in the measurement of the number of particles in our arrangement and for the increased ionization loss for a certain fraction of the electrons.

Since the measurement of the number of particles has been carried out under sufficiently thick lead absorbers (4.7 and 9.0 cm mean thickness) then the electron flux observed under the absorbers (in the differences  $N_4 - N_0$  and  $N_8 - N_{\text{HC}}$ ) contains a contribution from secondary penetrating particles produced in the first interaction between the "primary" particle and a lead nucleus. According to our estimates, secondary interactions increase the number of electrons under the absorber by 10% for  $t = 4.7 \text{ cm}$  and by 25% for  $t = 9.0 \text{ cm}$ . In addition, about 10% of detected particles represent penetrating particles produced in lead.

The corrected values of  $\epsilon_{\pi^0}^{\text{Pb}}$  are listed in Tables IV and V.

In Table IV (measurements at  $51^\circ$  geomagnetic latitude) and in Table V (at  $31^\circ$  geomagnetic latitude), the atmospheric depth in  $\text{g/cm}^2$  of the observation level is given in column 1, the mean thickness  $t$  of the lead absorber (under which the electron flux was measured) in column 2, the corrected electron flux in column 3, the energy transferred to  $\pi^0$  mesons per second in one gram of lead in column 4, the energy transferred to  $\pi^0$  mesons per second in one gram of air in column 5, the ratio  $E_{\pi^0}^{\text{Pb}}/E_{\pi^0}^{\text{Air}}$  (the energy transferred to  $\pi^0$  mesons in one act of interaction with a lead nucleus to that with an air nucleus) in column 6, and the mean weighted value of  $E_{\pi^0}^{\text{Pb}}/E_{\pi^0}^{\text{Air}}$  in column 7. All errors given are statistical.

TABLE IV

$x$ , g/cm <sup>2</sup>	$t$ , ra- dia- tion units	$n(t)$ cm <sup>-2</sup> sec <sup>-1</sup>	$\epsilon_{\pi^0}^{\text{Pb}}$ , Mev g <sup>-1</sup> sec <sup>-1</sup>	$\epsilon_{\pi^0}^{\text{Air}}$ Mev g <sup>-1</sup> sec <sup>-1</sup>	$E_{\pi^0}^{\text{Pb}}/E_{\pi^0}^{\text{Air}}$	Mean weighted value of $E_{\pi^0}^{\text{Pb}}/E_{\pi^0}^{\text{Air}}$
30	10	1.76±0.17	3.2±0.3	4.7±0.6	1.8±0.3	1.85±0.2
30	20	1.85±0.30	3.4±0.6	4.7±0.6	1.9±0.4	

TABLE V

$x$ , g/cm <sup>2</sup>	$t$ , ra- dia- tion units	$n(t)$ cm <sup>-2</sup> sec <sup>-1</sup>	$\epsilon_{\pi^0}^{\text{Pb}}$ Mev g <sup>-1</sup> sec <sup>-1</sup>	$\epsilon_{\pi^0}^{\text{Air}}$ Mev g <sup>-1</sup> sec <sup>-1</sup>	$E_{\pi^0}^{\text{Pb}}/E_{\pi^0}^{\text{Air}}$	Mean weighted value of $E_{\pi^0}^{\text{Pb}}/E_{\pi^0}^{\text{Air}}$
0*	10	2.5±0.3	4.6±0.6	5.5±0.3	2.2±0.3	2.4±0.2
20	10	1.9±0.2	3.6±0.3	3.8±0.2	2.5±0.3	
30	10	1.8±0.2	3.2±0.3	3.2±0.4	2.7±0.4	

\*The values for  $x = 0$  are obtained by means of extrapolation of the curves in Figs. 5 and 6.

It can be seen that  $E_{\pi^0}^{\text{Pb}}/E_{\pi^0}^{\text{Air}} = 2.4 \pm 0.2$  at 31° geomagnetic latitude, where the primary particles have an energy  $E_0 \geq 7$  Bev. At 51° geomagnetic latitude, where particles of lower energies down to 1.5 Bev are also present, the value of the ratio is  $1.85 \pm 0.2$ .

## 5. DISCUSSION OF RESULTS

### 1. Production of Heavily-Ionizing Particles in Air and in Light Substances

The range of most particles originating in stars is much smaller than the range of the star-producing component. It follows, therefore, that the number of particles stopping in one gram of the absorber should be equal to the number of particles produced in one gram of the absorber.

Let us denote by  $\nu_i$  the mean number of heavily-ionizing particles produced in the disintegration of one nucleus with mass number  $A_i$ . We shall denote further by  $N_{\text{stop}}(A_i)$  the number of particles stopping in one gram of the matter of an absorber of mass number  $A_i$ , and by  $N_{\text{stop}}^{\text{em}}(A_i)$  — the number of particles stopping in one gram of emulsion surrounded by the absorber. It follows from the equilibrium condition that

$$N_{\text{stop}}(A_i) = \nu_i N_{\text{star}}(A_i),$$

where  $N_{\text{star}}(A_i)$  is the number of stars produced in one gram of the matter of the absorber.

Heavily-ionizing particles are produced in the absorber, and stop in the emulsion. The power of the latter is  $\beta_{\text{em}}/\beta_i$  times larger than that of the absorber ( $\beta_{\text{em}}$  and  $\beta_i$  is the ionization loss in emulsion and in the absorber respectively) and we have, therefore

$$N_{\text{stop}}^{\text{em}}(A_i) = N_{\text{stop}}(A_i) \beta_{\text{em}}/\beta_i, \quad N_{\text{star}}^{\text{em}}(A_i) = \nu_i \beta_{\text{em}} N_{\text{star}}(A_i)/\beta_i.$$

The number of stars produced in one gram of the matter of the absorber can be expressed in terms of the number of stars produced in one gram of the emulsion surrounded by it:

$$N_{\text{star}}(A_i) = N_{\text{star}}^{\text{em}}(A_i) \sigma_i A_{\text{em}}/\sigma_{\text{em}} A_i = N_{\text{star}}^{\text{em}}(A_i) (A_{\text{em}}/A_i)^{1/3},$$

since the effective cross-section for star production is  $\sigma \sim A^{2/3}$  (reference 6). We have, therefore,

$$\nu_i = N_{\text{stop}}^{\text{em}}(A_i) \beta_i/N_{\text{star}}^{\text{em}}(A_i) \beta_{\text{em}} \left(\frac{A_i}{A_{\text{em}}}\right)^{1/3} \quad (7)$$

Taking the ratios of such expressions for lead and air and for graphite and air, and making use of the experimental data (Table III), we obtain

$$\nu_{\text{Pb}}/\nu_{\text{Air}} = 2.0 \pm 0.24;$$

$$\nu_{\text{C}}/\nu_{\text{Air}} = 0.82 \pm 0.10, \quad \text{at 20 km altitude}$$

It can be seen that, within the limits of experimental errors  $\nu \sim A^{1/3}$ .

### 2. Disintegration Energy of Light and Heavy Nuclei

According to Eqs. (1) and (2), we have

$$E_t = \frac{A}{Z} E_c = \frac{A}{Z} \frac{L_i}{S} \beta \int_{\Omega} d\Omega \int_{I_{\text{min}}}^{\infty} \frac{I}{I_{\text{rel}}} N(I, \theta) dI \quad (8)$$

$$= \frac{A}{Z} \frac{L_i}{S} \beta \bar{I} N_{\text{hi}},$$

where  $\bar{I}$  is the mean specific ionization of the flux of heavily ionizing particles, and  $N_{\text{hi}}$  is their total flux.

In our experiments,  $I_{\text{min}} = 2 I_{\text{rel}}$  (where  $I_{\text{rel}}$  is the specific ionization of a relativistic particle). For traversing particles,  $I \leq 12 I_{\text{rel}}$ . The remain-

ing particles stopped in the emulsion:

$$\bar{N}_{hi} = \bar{I}_{tr} N_{tr} + \bar{I}_{stop} N_{stop},$$

where  $\bar{I}_{tr}$  and  $\bar{I}_{stop}$  are the mean specific ionization of traversing and stopping particles, and  $N_{tr}$  and  $N_{stop}$  are their total fluxes, respectively.

We calculated the values of  $\bar{I}_{tr}$  and  $\bar{I}_{stop}$ , using the observed spectrum, corrected for geometry of the apparatus. The results, expressed in units of  $I_{rel}$ , are given in Table VI.

TABLE VI

Altitude, km	Absorber and its thickness, mm	$\bar{I}_{tr}$ (traversing particles)	$\bar{I}_{stop}$ (stopping particles)
20	Air	$5.8 \pm 0.3$	$18.2 \pm 1.7$
	Lead, 33	$4.7 \pm 0.3$	$21.3 \pm 2.3$
	Graphite, 86	$4.9 \pm 0.2$	$19.2 \pm 1.9$
9	Paraffin, 170	$6.3 \pm 0.4$	$20.8 \pm 1.7$
	Lead, 35	$6.1 \pm 0.4$	$20.8 \pm 1.6$

Using the data on the fluxes of the traversing and stopping particles (Table II) and the data of Table VI, we obtain the values of  $\bar{N}_{hi}$  for 20 km altitude.

In order to exclude the unknown flux of the generating component  $S$ , we form the ratios of Eq. (8) for the results of measurements under various absorbers. For the altitude of 20 km we find then that  $E_d^{Pb}/E_d^{Air} = 2.1 + 0.3$ , and  $E_p^C/E_p^{Air} = 0.82 + 0.08$ . Evidently, the disintegration energy  $E_d$  is proportional to  $A^{1/3}$ . We can conclude from the results on star production in substances with different atomic numbers that the mean number of particles in a star  $\nu$  and the mean disintegration energy of the nucleus  $\bar{E}_d$  are proportional to  $A^{1/3}$ , i.e., to the size of the nucleus.

### 3. Dependence of the Energy Carried Away by $\pi^0$ Mesons on the Mass Number of the Nucleus

A comparison of the energy carried away by  $\pi^0$  mesons in interactions involving lead and air nuclei shows (cf. Tables IV and V) that, in collisions with lead nuclei, primary particles with energy  $E_0 \geq 7$  BeV transfer to  $\pi^0$  mesons twice the amount of energy transferred in collisions with air nuclei. This result can be explained by the assumption that a collision of the "primary" particle with a heavy nucleus represents a series of collisions with lighter nuclei. The mean number of such collisions in the lead nucleus is  $n = (A_{Pb}/A_{Air})^{1/3} = 2.4$ .

We showed earlier<sup>2</sup> that a nucleon with  $E_0 \geq 7$  BeV colliding with air loses  $28 \pm 3\%$  of its primary energy on  $\pi$ -meson production. The remaining

72% of the energy is carried away by a single nucleon. Assuming the above collision model, a nucleon with  $E_0 \geq 7$  BeV should, in the mean, carry away an energy equal to  $(0.72 \pm 0.03)^{2.4} E_0 = (0.45 \pm 0.06) E_0$  in an interaction with a lead nucleus. Consequently,  $E_{\pi^0}^{Pb}/E_0 = 55 + 6\%$  of the primary energy will be spent on  $\pi$ -meson production in lead, and  $E_{\pi^0}^{Air}/E_0 = 28 + 3\%$  in air.

It is natural to assume that the energy carried away by  $\pi^0$  mesons is half the energy carried away by  $\pi^+$  mesons, in collisions with both light and heavy nuclei. We should have then

$$E_{\pi^0}^{Pb}/E_{\pi^0}^{Air} = \frac{(55 \pm 6)\%}{(28 \pm 3)\%} = 2.0 \pm 0.3.$$

It can be concluded, therefore, that the energy carried away by  $\pi^0$  mesons varies roughly in proportion to the size of the nucleus, i.e.,  $E_{\pi^0} \sim A^{1/3}$ .

### CONCLUSIONS

1. In interactions between  $\sim 10$  BeV nucleons and atomic nuclei, the disintegration energy  $E_d$  and the energy carried away by the  $\pi^0$  mesons are proportional to the size of the nucleus, i.e.,

$$E_d \sim A^{1/3}, \quad E_{\pi^0} \sim A^{1/3}.$$

2. The observed dependence of  $E_d$  and  $E_{\pi^0}$  on  $A$  is consistent with the assumption that an interaction between a primary particle and a heavy nucleus represents a succession of independent interactions of a similar type to that with a lighter nucleus, e.g., an air nucleus. The mean number of these independent interactions is proportional to  $\sim A^{1/3}$ .

<sup>1</sup> N. L. Grigorov and V. S. Murzin, *Izv. Akad. Nauk, SSSR, Ser. Fiz.* **17**, 21 (1953).

<sup>2</sup> N. L. Grigorov, *Usp. Fiz. Nauk*, **58**, 599 (1956).

<sup>3</sup> U. Camerini and C. F. Powell, *Usp. Fiz. Nauk* **40**, 76 (1950).

<sup>4</sup> S. I. Brikker and N. L. Grigorov, *Dokl. Akad. Nauk SSSR* **86**, 1089 (1952).

<sup>5</sup> Grigorov, Rapoport, and Shipulo, *Dokl. Akad. Nauk SSSR* **91**, 491 (1953).

<sup>6</sup> I. Barbour, *Phys. Rev.* **82**, 280 (1951).